Thermal properties of surface and bulk spin waves in uniaxial and nonuniaxial metamagnetic films

E. Meloche and M. G. Cottam*
Department of Physics and Astronomy, University of Western Ontario, London, Ontario, Canada N6A 3K7
(Received 14 April 2004; published 28 September 2004)

A theory is presented for the temperature dependence of surface and bulk spin waves in metamagnetic films, allowing for the inclusion of both uniaxial and nonuniaxial contributions to the single-ion anisotropy. A Green's function formalism is employed to evaluate spin-wave dispersion relations and the mean square amplitudes of spin-wave modes. The theory is applied to obtain numerical results for the $S=1$ metamagnets $FeBr_2$ and $FeCl_2$ in both the antiferromagnetic and ferromagnetic phases, depending on the strength of the applied magnetic field. The case of ultrathin films with a relatively small number of atomic layers is considered, as well as that of thicker films.

DOI: 10.1103/PhysRevB.70.094423 PACS number(s): 75.30.Ds, 75.70.−i

I. INTRODUCTION

In recent years there have been numerous theoretical and experimental studies of spin waves in antiferromagnetic (AFM) and ferromagnetic (FM) thin films (see Refs. 1–3 for reviews). In some bulk magnetic materials, light scattering experiments have clearly demonstrated that higher-frequency (or optical) spin waves can occur in the spectrum at elevated temperatures in addition to the usual (or acoustic) spin waves seen at lower temperatures.[4] These optical spin waves are attributed to the single-ion anisotropy and correspond to transitions between higher magnetic states, which can therefore become important at higher temperatures when the states become populated. Many of the theoretical works on ordered magnetic materials with large single-ion anisotropy, such as metamagnets, have been limited to the low-temperature regime ($T \ll T_c$), in which the anisotropy can be represented to a good approximation as an effective anisotropy field (as in Refs. 5 and 6). This simplification becomes unsatisfactory when considering results over a broader range of temperatures, partly because of the problem of specifying the temperature dependence of the effective anisotropy field but also because it leads to a simplication of the spin dynamics by neglecting optical magnons.

In this paper we investigate the effects of both uniaxial and nonuniaxial single-ion anisotropy on the thermal properties of spin-wave excitations in metamagnetic films. Within a Green's function equation-of-motion method, we extend previous theoretical studies on metamagnets by treating the anisotropy terms exactly. Thermal effects are introduced by considering layer-dependent static thermal averages for the spins. The method involves generating a closed set of coupled equations for all of the required Green's functions, using the random phase approximation (RPA) to linearize only the exchange terms. Explicit expressions for the Green's functions are obtained by solving an inhomogenous matrix equation. From the Green's functions we are then able to extract dispersion relations and evaluate the spin-dependent correlation functions, which are of interest since they determine the dynamic response of the magnetic system. It is shown that the inclusion of thermal effects leads to additional optical surface and bulk spin-wave modes that become important at elevated temperatures.

Spin-wave dispersion relations in semi-infinite metamagnetic materials (considering only one surface) have been reported, but these were limited to the low-temperature ($T \ll T_c$) regime.[5] The dispersion relations were obtained using an operator equation-of-motion approach, and the anisotropy (taken as uniaxial) was treated as an effective field. Some limited low-temperature properties of surface and bulk spin waves in metamagnets with nonuniaxial single-ion anisotropy have been reported (see Ref. 6). Again, these results were also obtained using an effective-field approximation to represent the uniaxial and nonuniaxial anistropy. Recently we reported some temperature-dependent results for spin-wave properties in semi-infinite metamagnets.[7] In these preliminary results we considered only the contribution of the uniaxial part of the single-ion anisotropy and ignored finite film thickness effects.

In general, metamagnets consist of ferromagnetically ordered layers that are weakly coupled by AFM exchange to adjacent layers. In the presence of a weak external field H_0 (applied perpendicular to the layers) the overall ordering of adjacent layers is antiparallel, giving the AFM phase. If the applied field is large enough to overcome the AFM interlayer coupling, spins in adjacent layers will order parallel to one another, giving the FM phase. There is no intermediate spin-flop phase, as in normal antiferromagnets, because of the large anisotropy. In this paper we consider spin-wave properties in both phases and apply the theory to obtain numerical results for films of the metamagnets $FeBr_2$ and $FeCl_2$ over a wide range of temperatures below T_c.

The outline of the paper is as follows. In Sec. II we describe the metamagnetic Hamiltonian and the general Green's function formalism for $S=1$ systems. In Sec. III we describe the theory for a uniaxial metamagnet and outline the method used to obtain explicit expressions for the Green's functions in both the FM and AFM phases. This is followed in Sec. IV with the theory for metamagnets with nonuniaxial contributions to the anisotropy in both the FM and AFM phases. In Sec. V we apply the theory to obtain numerical results for dispersion relations and the mean-square amplitudes (as a measure of intensity) of surface and bulk spin-wave modes in $FeBr_2$ and $FeCl_2$. The final section, Sec. VI, contains the conclusions of our work.

II. HAMILTONIAN AND BASIC FORMALISM

We represent the $S=1$ metamagnets by the following spin Hamiltonian:

$$H = \sum_{i,j} J_{i,j}(\mathbf{S}_i \cdot \mathbf{S}_j + \sigma S_i^z S_j^z) + H_Z + H_A - \frac{1}{2}\sum_{i,i'} J'_{i,i'}(\mathbf{S}_i \cdot \mathbf{S}_{i'} + \sigma' S_i^z S_{i'}^z) - \frac{1}{2}\sum_{j,j'} J'_{j,j'}(\mathbf{S}_j \cdot \mathbf{S}_{j'} + \sigma' S_j^z S_{j'}^z), \quad (1)$$

where the Zeeman term is given by

$$H_z = -g\mu_B H_0\left(\sum_i S_i^z + \sum_j S_j^z\right), \quad (2)$$

and the single-ion anisotropy is represented in general by

$$H_A = -D\left[\sum_i (S_i^z)^2 + \sum_j (S_j^z)^2\right] - F\left[\sum_i (S_i^x)^2 - (S_i^y)^2\right] - F\left[\sum_j (S_j^x)^2 - (S_j^y)^2\right]. \quad (3)$$

The term $J_{i,j}$ is the weaker interlayer AFM exchange between sites i and j on different sublattices, while $J'_{i,i}$ and $J'_{j,j}$ are the stronger FM intralayer exchanges. The possibility of exchange anisotropy (of the Ising type) is represented by parameters σ and σ'. The applied field H_0 is taken to be in the z direction, which is perpendicular to the layers. The parameters D and F describe the effects of the uniaxial and nonuniaxial contributions to the anisotropy, respectively.

We consider a N-layer metamagnetic film with a pair of surfaces in the (001) direction. The layers are labeled using a positive index n, with $n=1$ and $n=N$ denoting the two surfaces. In the AFM phase we assume that the spins in layers with an odd (even) layer index n belong to the spin-up (down) sublattice and have a thermal average $\langle S^z\rangle$ positive (negative). Thus, while the top $n=1$ surface layer belongs to the spin-up sublattice, the lower surface at $n=N$ may be either on the spin-up or spin-down sublattice, depending on whether N is odd or even. We anticipate that this odd/even property will have consequences for the spin-wave spectrum.

The spin-dependent Green's functions are obtained following an equation-of-motion approach (see Ref. 8). The method involves writing down the equation of motion for each of the required Fourier transformed Green's functions using

$$\omega\langle\langle X;Y\rangle\rangle_\omega = \left(\frac{1}{2\pi}\right)\langle[X,Y]\rangle + \langle\langle[X,H];Y\rangle\rangle_\omega, \quad (4)$$

where $[X,Y]$ is the commutator between operators X and Y, and $\langle\cdots\rangle$ represents a static thermal average.

We begin by forming the equation of motion for the transverse Green's function of the form $\langle\langle S_l^+;S_m^-\rangle\rangle_\omega$ at general sites labeled l and m within the film. This leads to more complicated Green's functions being generated on the right-hand side of the expression. The Green's functions arising from the exchange terms in the Hamiltonian H involve products of operators at different sites and are decoupled using the RPA. The single-ion anisotropy term in Hamiltonian gives rise to Green's function involving the product of operators at the same sites and are not decoupled. They are treated exactly by forming new equations of motion in order to form a closed set of equations. The system of equations is then transformed to a wave vector representation and the transformed Green's functions are obtain using standard mathematical procedures. The Green's functions provide information about dispersion relations and spectral intensities of the magnons. This method has been applied to study light scattering from bulk magnons in various anisotropic antiferromagnets and ferromagnets and, in principle, can be used for any value of the spin S. This approach is particular suitable for low spin values because the number of equations of motion needed to form a closed set is then relatively small. In this work we present results for metamagnetic materials such as $FeBr_2$ and $FeCl_2$ with spin $S=1$.

We expect one acoustic and one optical magnon in this case. A simple argument to see this is to consider just the single-ion term in H, which gives rise to three unequally spaced energy levels when $S=1$. Transitions between adjacent levels can therefore occur between either the lower pair or the upper pair, leading to acoustic and optical magnons when the full form of H is taken into account. These main branches can each be split into two by an applied field in the AFM phase, and in our film geometry we expect to find surface and bulk modes.

III. THEORY FOR UNIAXIAL CASE

For simplicity, we begin by considering the uniaxial case ($F=0$). Substituting the operators X and Y in Eq. (4) with the spin operators S_l^+ and S_m^- respectively, we form the equation of motion for the $\langle\langle S_l^+;S_m^-\rangle\rangle_\omega$ Green's function. We linearize the equation of motion using standard RPA, which decouples the product of operators at different sites. The linearized equation of motion for $F_{lm}(\omega)\equiv\langle\langle S_l^+;S_m^-\rangle\rangle_\omega$ is written as

$$\left[E_0 + (1+\sigma)\sum_i J_{i,l}m_i - (1+\sigma')\sum_i J'_{i,l}m_i\right]F_{lm}(\omega) = (1/\pi)m_l\delta_{l,m} + DG_{lm}(\omega) + m_l\left[\sum_i J_{i,l}F_{im}(\omega) - \sum_i J'_{i,l}F_{im}(\omega)\right], \quad (5)$$

where $E_0=\omega-g\mu_B H_0$. The uniaxial anisotropy leads to a Green's function of the form $G_{lm}(\omega)\equiv\langle\langle S_l^+S_l^z+S_l^zS_l^+;S_m^-\rangle\rangle_\omega$, which is not decoupled because it involves the product of operators at the same site. The linearized equation of motion for this Green's function is

$$\left[E_0 + (1+\sigma)\sum_i J_{i,l}m_i - (1+\sigma')\sum_i J'_{i,l}m_i\right]G_{lm}(\omega) = (1/\pi)M_l\delta_{l,m} + DF_{lm}(\omega) + M_l\left[\sum_i J_{i,l}F_{im}(\omega) - \sum_i J'_{i,l}F_{im}(\omega)\right]. \quad (6)$$

The expressions involve static thermal averages $\langle S_l^z\rangle$ and $3\langle(S_l^z)^2\rangle-2$, which we have denoted by m_l and M_l, respectively.

Next we exploit the translational symmetry parallel to the layers and Fourier transform the linearized coupled equations of motion to a wave vector representation using

$$F_{lm}(\omega) = \frac{1}{N_1}\sum_{\mathbf{k}_\parallel} \mathbf{F}_{n,n'}(\mathbf{k}_\parallel,\omega)\exp[i\mathbf{k}_\parallel\cdot(\vec{r}_l-\vec{r}_m)], \tag{7}$$

where $\mathbf{k}_\parallel=(k_x,k_y)$ is a two-dimensional wave vector parallel to the surface, $\vec{r}$ is a position vector, and N_1 is the number of sites in any layer. We employ a similar transformation for $G_{lm}(\omega)$ and denote its Fourier components as $\mathbf{G}_{n,n'}(\mathbf{k}_\parallel,\omega)$. The indices n and n' label the layers parallel to the surface. We also introduce Fourier transforms for the intralayer exchange interaction, which we write as

$$u(\mathbf{k}_\parallel) = \sum_i J'_{i,i'}\exp[i\mathbf{k}_\parallel\cdot(\mathbf{r}_i-\mathbf{r}_{i'})], \tag{8}$$

and for the interlayer exchange interaction we write

$$v(\mathbf{k}_\parallel) = \sum_{\boldsymbol{\delta}} J_{i,j}(\boldsymbol{\delta})\exp(i\mathbf{k}_\parallel\cdot\boldsymbol{\delta}), \tag{9}$$

where vector $\boldsymbol{\delta}$ joins sites in layer n to sites in layer $n+1$.

The transformed equations of motion for $\mathbf{F}_{n,n'}(\mathbf{k}_\parallel,\omega)$ and $\mathbf{G}_{n,n'}(\mathbf{k}_\parallel,\omega)$ are

$$[E_n + m_n u(\mathbf{k}_\parallel)]\mathbf{F}_{n,n'} - m_n[v(-\mathbf{k}_\parallel)\mathbf{F}_{n-1,n'} + v(\mathbf{k}_\parallel)\mathbf{F}_{n+1,n'}] - D\mathbf{G}_{n,n'} = \frac{1}{\pi}m_n\delta_{n,n'}, \tag{10}$$

$$E_n\mathbf{G}_{n,n'} = \frac{1}{\pi}M_n\delta_{n,n'} + M_n[v(-\mathbf{k}_\parallel)\mathbf{F}_{n-1,n'} + v(\mathbf{k}_\parallel)\mathbf{F}_{n+1,n'}] + [D - M_n u(\mathbf{k}_\parallel)]\mathbf{F}_{n,n'}, \tag{11}$$

where

$$E_n = [E_0 + (1+\sigma)(m_{n-1}+m_{n+1})v(0) - (1+\sigma')m_n u(0)]. \tag{12}$$

From symmetry considerations it is clear that the thermal averages m_l and M_l depend on position only through the layer index n. We estimate the layer-dependent thermal averages m_n and M_n using a modified mean-field theory which we describe in the Appendix. Substituting Eq. (11) into Eq. (10) reduces the system to a single equation of motion for the $\mathbf{F}_{n,n'}(\mathbf{k}_\parallel,\omega)$ Green's functions. We now describe the formalism used to obtain the Green's functions in each phase.

A. The ferromagnetic phase

The critical field $H_c(T)$ producing a transition from the AFM to the FM phase in bulk metamagnets is given approximately[5] in the low-temperature limit by

$$g\mu_B H_c(0) = 2(1+\sigma)Sv(0). \tag{13}$$

At higher temperatures we will find its value numerically.

The analysis in the FM phase ($H_0 > H_c$) is straightforward because all of the spins are aligned in the direction of the applied field H_0 and belong to the same sublattice. If we consider a metamagnetic film composed of N layers, the closed set of finite difference equations is

$$\begin{aligned}
&f_1\mathbf{F}_{1,n'} - v(\mathbf{k}_\parallel)\mathbf{F}_{2,n'} = (1/\pi)\delta_{1,n'}, \quad n=1,\\
&-v(-\mathbf{k}_\parallel)\mathbf{F}_{1,n'} + f_2\mathbf{F}_{2,n'} - v(\mathbf{k}_\parallel)\mathbf{F}_{3,n'} = (1/\pi)\delta_{2,n'}, \quad n=2,\\
&-v(-\mathbf{k}_\parallel)\mathbf{F}_{n-1,n'} + f_n\mathbf{F}_{n,n'} - v(\mathbf{k}_\parallel)\mathbf{F}_{n+1,n'} = (1/\pi)\delta_{n,n'}, \quad n=3,\ldots,N-2,\\
&-v(-\mathbf{k}_\parallel)\mathbf{F}_{N-2,n'} + f_{N-1}\mathbf{F}_{N-1,n'} - v(\mathbf{k}_\parallel)\mathbf{F}_{N,n'} = (1/\pi)\delta_{N-1,n'}, \quad n=N-1,\\
&-v(-\mathbf{k}_\parallel)\mathbf{F}_{N-1,n'} + f_N\mathbf{F}_{N,n'} = (1/\pi)\delta_{N,n'}, \quad n=N,
\end{aligned} \tag{14}$$

where

$$f_n = [A_nB_n - D(D-M_n)]/(m_nB_n + DM_n). \tag{15}$$

The parameters appearing in (15) are

$$\begin{aligned}
A_1 &= E_0 + (1+\sigma)mv(0) - (1+\sigma')m_1u(0) + m_1u(\mathbf{k}_\parallel),\\
A_2 &= E_0 + (1+\sigma)(m_1+m)v(0) - (1+\sigma')mu(0) + mu(\mathbf{k}_\parallel),\\
A_n &= E_0 + 2(1+\sigma)mv(0) - (1+\sigma')mu(0) + mu(\mathbf{k}_\parallel), \quad n=3,\ldots,N-2,\\
A_{N-1} &= E_0 + (1+\sigma)(m_N+m)v(0) - (1+\sigma')mu(0) + mu(\mathbf{k}_\parallel),\\
A_N &= E_0 + (1+\sigma)mv(0) - (1+\sigma')m_Nu(0) + m_Nu(\mathbf{k}_\parallel),
\end{aligned} \tag{16}$$

and $B_n = A_n - m_nu(\mathbf{k}_\parallel)$. In writing (15) and (16) we use the approximation that only the thermal averages for the surface layers ($n=1$ and $n=N$) are significantly different from those for interior layers. Specifically, we denote m_n as m_1 for $n=1$, m_N for $n=N$, and the bulk value m otherwise. A similar notation is used for M_n.

The system of finite difference equations can be expressed in matrix form as

$$\mathbf{A}\mathbf{F}_{n'} = \mathbf{b}_{n'}, \tag{17}$$

where $\mathbf{F}_{n'}$ and $\mathbf{b}_{n'}$ are N-component column matrices with elements given by $(\mathbf{F}_{n'})_n = F_{n,n'}$ and $(\mathbf{b}_{n'})_n = 1/(\pi|v(\mathbf{k}_\parallel)|)\delta_{n,n'}$.

Following the general approach used in Ref. 9 for thin films, which is an extension of earlier calculations for semi-infinite samples, we split the $N\times N$ matrix $\mathbf{A}$ into two parts such that $\mathbf{A}=\mathbf{A}_0+\boldsymbol{\Delta}$. Here the matrix $\mathbf{A}_0$, which is a tridiagonal matrix containing only bulk parameters of the film, has its nonzero elements defined as $(\mathbf{A}_0)_{i,i}=d$ and $(\mathbf{A}_0)_{i,i\pm1}=-\tau^{\mp1}$, where

$$d = f_n/(|v(\mathbf{k}_\parallel)|) \text{ and } \tau = \sqrt{v(-\mathbf{k}_\parallel)/v(\mathbf{k}_\parallel)}. \tag{18}$$

Matrix $\boldsymbol{\Delta}$, which describes the perturbation due to the surface, has only a few nonzero elements, namely,

$$\Delta_{i,i} = (f_i - f_n)/|v(\mathbf{k}_\parallel)|, \tag{19}$$

for $i=1,2,N-1,N$. This decomposition is helpful because the inverse of $\mathbf{A}_0$ is known.[15] Denoting $\mathbf{B}=\mathbf{A}_0^{-1}$, the result is

$$B_{i,j} = \begin{cases} \tau \dfrac{\{\tau^{2i}x^{i+j} - x^{j-i} + (\tau^2)^{N+1-j}x^{2N+2-(i+j)} - (\tau^2)^{N+1-(j-i)}x^{2N+2-(j-i)}\}}{(\tau^2 x - x^{-1})(1-(\tau x)^{2N+2})}, & i \leqslant j \\ \tau \dfrac{\{\tau^{2i}x^{i+j} - (\tau^2)^{i-j}x^{i-j} + (\tau^2)^{N+1-j}x^{2N+2-(i+j)} - (\tau^2)^{N+1}x^{2N+2-(i-j)}\}}{(\tau^2 x - x^{-1})[1-(\tau x)^{2N+2}]}, & i > j, \end{cases} \tag{20}$$

where the complex parameter x is defined by $\tau x + 1/(\tau x) = d$ and satisfies the condition $|x| \leqslant 1$.

The formal solution of Eq. (17) is written as

$$\mathbf{F}_{n'} = (\mathbf{I} + \mathbf{B\Delta})^{-1}\mathbf{B}\mathbf{b}_{n'}, \tag{21}$$

where $\mathbf{I}$ denotes the $N \times N$ unit matrix. It is then necessary to invert the matrix $(\mathbf{I}+\mathbf{B\Delta})$, which can be written in partitioned form as

$$(\mathbf{I} + \mathbf{B\Delta}) = \begin{pmatrix} M_1 & 0 & M_6 \\ M_2 & \mathbf{I} & M_5 \\ M_3 & 0 & M_4 \end{pmatrix}, \tag{22}$$

where M_1, M_3, M_4, and M_6 are 2×2 matrices, whereas M_2 and M_5 are $2 \times (N-4)$ matrices. The required inverse can also be written in partitioned form as

$$(\mathbf{I} + \mathbf{B\Delta})^{-1} = \begin{pmatrix} X_1 & 0 & X_6 \\ X_2 & \mathbf{I} & X_5 \\ X_3 & 0 & X_4 \end{pmatrix}, \tag{23}$$

with elements given by

$$\begin{aligned} X_1 &= -(M_3 - M_4M_6^{-1}M_1)^{-1}M_4M_6^{-1}, \\ X_2 &= -M_5M_6^{-1} + (M_5M_6^{-1}M_1 - M_2)X_1, \\ X_3 &= M_6^{-1} - M_6^{-1}M_1X_1, \\ X_4 &= -M_6^{-1}M_1(M_3 - M_4M_6^{-1}M_1)^{-1}, \\ X_5 &= (M_5M_6^{-1}M_1 - M_2)(M_3 - M_4M_6^{-1}M_1)^{-1}, \\ X_6 &= (M_3 - M_4M_6^{-1}M_1)^{-1}. \end{aligned} \tag{24}$$

The explicit expressions for all of the Green's functions $\mathbf{F}_{n,n'}(\mathbf{k}_\parallel, \omega)$ can be obtained by carrying out the appropriate matrix multiplications on the right-hand side of Eq. (21). The spin-wave energies are found from the poles of these Green's functions. We shall find in the application presented later that the solutions for a thin-film geometry, which consist of quantized bulk modes and some discrete surface modes, come from the $(\mathbf{I}+\mathbf{B\Delta})^{-1}$ term; i.e., they correspond to solutions of

$$\det(\mathbf{I} + \mathbf{B\Delta}) = 0. \tag{25}$$

From the diagonal Green's functions $\mathbf{F}_{n,n}(\mathbf{k}_\parallel, \omega)$ and the use of the fluctuation-dissipation theorem, we write the spectral intensity of the spin-wave modes in layer n and wave vector $\mathbf{k}_\parallel$ as $\xi_n(\mathbf{k}_\parallel, \omega)$, which we define as

$$\xi_n(\mathbf{k}_\parallel, \omega) = \frac{-2}{\exp(\beta\omega) - 1}\mathrm{Im}\{\mathbf{F}_{n,n}(\mathbf{k}_\parallel, \omega + i\eta)\}, \tag{26}$$

where $\beta = 1/k_BT$, k_B is the Boltzmann constant and T the temperature. The real and positive quantity η is introduced phenomenologically to model an intrinsic damping or reciprocal lifetime. The above spectral intensities are used to evaluate equal-time correlation functions, which in turn are used to find the layer-dependent mean-square amplitude of spin precession defined as

$$Q(n) = \langle (S_n^x)^2 + (S_n^y)^2 \rangle_{\mathbf{k}_\parallel}. \tag{27}$$

In the numerical examples presented in Sec. V we will find that the optical modes have spectral functions and mean-square amplitudes that vanish in the low-temperature limit but become important at elevated temperatures.

B. The antiferromagnetic phase

The analysis is algebraically more complicated in the AFM phase $(H_0 < H_c)$ because spins in adjacent layers belong to different sublattices. The thermal averages associated with an odd layer index n belong to the spin-up sublattice, whereas those associated with an even layer index n belong the spin-down sublattice.

The set of finite difference equations are analogous to those in the FM phase, except now the coefficients of the diagonal Green's functions are defined as

$$f_n = [A_nB_n - D(D - M_n)]/[(-1)^{n+1}m_nB_n + DM_n]. \tag{28}$$

The parameters appearing in Eq. (28) are defined as

$$\begin{aligned} A_1 &= E_0 - (1+\sigma)mv(0) - (1+\sigma')m_1u(0) + m_1u(\mathbf{k}_\parallel), \\ A_2 &= E_0 + (1+\sigma)(m_1+m)v(0) + (1+\sigma')mu(0) - mu(\mathbf{k}_\parallel), \\ A_n &= E_0 + (-1)^n[2(1+\sigma)mv(0) + (1+\sigma')mu(0) \\ &\quad - mu(\mathbf{k}_\parallel)], \quad n = 3, \ldots, N-2, \\ A_{N-1} &= E_0 + (-1)^{N-1}\big[(1+\sigma)(m_N+m)v(0) + (1+\sigma')mu(0) \\ &\quad - mu(\mathbf{k}_\parallel)\big], \\ A_N &= E_0 + (-1)^N[(1+\sigma)mv(0) + (1+\sigma')m_Nu(0) - m_Nu(\mathbf{k}_\parallel)], \end{aligned} \tag{29}$$

and $B_n = A_n - (-1)^n m_n u(\mathbf{k}_\parallel)$. Here we again use the approximation that only the thermal averages for the surface layers $(n=1$ and $n=N)$ are different from those for interior bulk layers.

As a result of the two-sublattice system, we must treat the cases of N odd and N even differently. We first describe the approach used to obtain the Green's functions $\mathbf{F}_{n,n'}$ for a film with an *odd* number of layers. The Green's function associated with n odd (denoting $n=2\mu+1$) can be eliminated by substituting

$$\mathbf{F}_{1,n'} = [v(\mathbf{k}_\parallel)\mathbf{F}_{2,n'} + (1/\pi)\delta_{1,n'}]/f_1,$$

$$\mathbf{F}_{2\mu+1,n'} = [v(-\mathbf{k}_\parallel)\mathbf{F}_{2\mu,n'} + v(\mathbf{k}_\parallel)\mathbf{F}_{2\mu+2,n'} + (1/\pi)\delta_{2\mu+1,n'}]/f_{2\mu+1},\ \mu = 1, \ldots, (N-3)/2, \tag{30}$$

$$\mathbf{F}_{N,n'} = [v(\mathbf{k}_\parallel)\mathbf{F}_{N-1,n'} + (1/\pi)\delta_{N,n'}]/f_N,$$

into the equations for n even. The resulting system of equations is again written in matrix form as $\mathbf{A}\mathbf{F}_{n'}=\mathbf{b}_{n'}$ except now $\mathbf{F}_{n'}$ and $\mathbf{b}_{n'}$ are column matrices with $(N-1)/2$ elements defined as $(\mathbf{F}_{n'})_{2\mu}=\mathbf{F}_{2\mu,n'}$ and

$$(\mathbf{b}_{n'})_2 = (1/\pi)\Gamma[\delta_{2,n'} + (v(-\mathbf{k}_\parallel)/f_1)\delta_{1,n'} + (v(\mathbf{k}_\parallel)/f_{2\mu+1})\delta_{3,n'}],$$

$$(\mathbf{b}_{n'})_{2\mu} = (1/\pi)\Gamma[\delta_{2\mu,n'} + (v(-\mathbf{k}_\parallel)/f_{2\mu+1})\delta_{2\mu-1,n'} + (v(\mathbf{k}_\parallel)/f_{2\mu+1})\delta_{2\mu+1,n'}], \quad \mu = 2, \ldots, (N-3)/2, \tag{31}$$

$$(\mathbf{b}_{n'})_{N-1} = (1/\pi)\Gamma[\delta_{N-1,n'} + (v(-\mathbf{k}_\parallel)/f_{2\mu+1})\delta_{N-2,n'} + (v(\mathbf{k}_\parallel)/f_N)\delta_{N,n'}],$$

where $\Gamma = f_{2\mu+1}/|v(\mathbf{k}_\parallel)|^2$.

Following the approach used in the FM phase, we write the matrix $\mathbf{A}$ as the sum of $\mathbf{A}_0$ and Δ. The elements of $\mathbf{A}_0$ now correspond to

$$d = \Gamma f_{2\mu} - 2 \ \text{ and } \ \tau = v(-\mathbf{k}_\parallel)/v(\mathbf{k}_\parallel), \tag{32}$$

and matrix Δ now has just two nonzero elements

$$\Delta_{1,1} = \Gamma(f_2 - f_{2\mu}) - (f_{2\mu+1}/f_1) + 1,$$

$$\Delta_{N,N} = \Gamma(f_{N-1} - f_{2\mu}) - (f_{2\mu+1}/f_N) + 1. \tag{33}$$

For a film with an *even* number of layers, we also begin by eliminating the Green's functions associated with an odd layer index n. In this case the column matrices $\mathbf{F}_{n'}$ and $\mathbf{b}_{n'}$ have $N/2$ elements, and as a result of the surface layer $n=N$ belonging to the spin-down sublattice the elements $\mathbf{b}_{n'}$ are modified [see Eq. (35)].

The elements of the matrix $\mathbf{A}_0$ are defined as in the case of N odd, but the nonzero elements of $\mathbf{\Delta}$ are now

$$\Delta_{1,1} = (f_2 - f_{2\mu})\Gamma - (f_{2\mu+1}/f_1) + 1,$$

$$\Delta_{N-1,N-1} = 1 - (f_{2\mu+1}/f_{N-1}),$$

$$\Delta_{N-1,N} = \tau^{-1}\Delta_{N-1,N-1}, \tag{34}$$

$$\Delta_{N,N} = [f_N f_{N-1}/|v(\mathbf{k}_\parallel)|^2] - f_{2\mu}\Gamma + 1.$$

In both cases the solutions for the Green's functions $\mathbf{F}_{2\mu,n'}$ are obtained by inverting the matrix $\mathbf{A}$ following the same approach as in the FM phase. The solutions for the Green's functions $\mathbf{F}_{2\mu+1,n'}$ are then found from the set of finite difference equations. As before, the bulk and surface spin-wave modes are solutions of the determinantal condition in Eq. (25), and the mean-square amplitudes are calculated using Eq. (27):

$$(\mathbf{b}_{n'})_2 = (1/\pi)\Gamma[\delta_{2,n'} + (v(-\mathbf{k}_\parallel)/f_1)\delta_{1,n'} + (v(\mathbf{k}_\parallel)/f_{2\mu+1})\delta_{3,n'}],$$

$$(\mathbf{b}_{n'})_{2\mu} = (1/\pi)\Gamma[\delta_{2\mu,n'} + (v(-\mathbf{k}_\parallel)/f_{2\mu+1})\delta_{2\mu-1,n'} + (v(\mathbf{k}_\parallel)/f_{2\mu+1})\delta_{2\mu+1,n'}],\ \mu = 2, \ldots, (N-4)/2,$$

$$(\mathbf{b}_{n'})_{N-2} = (1/\pi)\Gamma[\delta_{N-2,n'} + (v(-\mathbf{k}_\parallel)/f_{2\mu+1})\delta_{N-3,n'} + (v(\mathbf{k}_\parallel)/f_{N-1})\delta_{N-1,n'}], \tag{35}$$

$$(\mathbf{b}_{n'})_N = (1/\pi)(f_{N-1}/|v(\mathbf{k}_\parallel)|^2)[\delta_{N,n'} + (v(-\mathbf{k}_\parallel)/f_{N-1})\delta_{N-1,n'}].$$

IV. THEORY FOR NONUNIAXIAL CASE

The calculations become more complicated when the nonuniaxial anisotropy ($F \neq 0$) is included, and for this reason we limit our analysis in this section to a semi-infinite metamagnet that occupies the half-space $z \leqslant 0$.

In the nonuniaxial case we must form the equations of motion of the Green's functions $\ll S_l^+; S_m^- \gg_\omega$, $\ll S_l^-; S_m^- \gg_\omega$, $\ll S_l^+ S_l^z + S_l^z S_l^+; S_m^- \gg_\omega$, and $\ll S_l^- S_l^z + S_l^z S_l^-; S_m^- \gg_\omega$ to obtain a closed set after applying RPA to the exchange terms. As before, the equations of motion are transformed to a representation involving layer indices and a two-dimensional wave vector parallel to the surface. This leads to four sets of equations coupling the various layer-dependent Fourier components. After tedious algebraic manipulations we can eliminate the Fourier components associated with $\ll S_l^+ S_l^z + S_l^z S_l^+; S_m^- \gg_\omega$ and $\ll S_l^- S_l^z + S_l^z S_l^-; S_m^- \gg_\omega$ and reduce the system to two sets of coupled equations, which we write as

$$\begin{aligned} &\Lambda_1 \mathbf{\Phi}_{1,n'} - v(\mathbf{k}_\parallel)\Theta_1 \mathbf{\Phi}_{2,n'} = (1/\pi)\Omega_1 \delta_{1,n'}, \quad n = 1, \\ &-v(-\mathbf{k}_\parallel)\Theta_n \mathbf{\Phi}_{n-1,n'} + \Lambda_n \mathbf{\Phi}_{n,n'} - v(\mathbf{k}_\parallel)\Theta_n \mathbf{\Phi}_{n+1,n'} \\ &\quad = (1/\pi)\Omega_n \delta_{n,n'}, \quad n > 1. \end{aligned} \tag{36}$$

Here $\mathbf{\Phi}_{n,n'}$ are two-component column vectors defined as

$$\mathbf{\Phi}_{n,n'} = \begin{pmatrix} \mathbf{F}^+_{n,n'}(\mathbf{k}_\parallel, \omega) \\ \mathbf{F}^-_{n,n'}(\mathbf{k}_\parallel, \omega) \end{pmatrix}, \tag{37}$$

where $\mathbf{F}^+_{n,n'}(\mathbf{k}_\parallel, \omega)$ and $\mathbf{F}^-_{n,n'}(\mathbf{k}_\parallel, \omega)$ represent the Fourier components of $\ll S_l^+; S_m^- \gg_\omega$ and $\ll S_l^-; S_m^- \gg_\omega$ respectively. The elements of the 2×2 matrices Λ_n and Θ_n and the column vectors Ω_n are complicated expressions involving frequency and the parameters of the metamagnetic materials. These expressions also involve the layer-dependent thermal average $<(S^+)^2>_n$, which we estimate numerically using a modified mean-field theory described in the Appendix. We again use

the approximation that only the thermal averages for the surface layer are significantly different from those for interior layers.

As in the uniaxial case, the analysis for the FM phase is simpler because all of the spins belong to one sublattice. The system of equations can be expressed in supermatrix form as $(\mathbf{A}_0+\mathbf{\Delta})\mathbf{\Phi}_{n'}=\mathbf{b}_{n'}$, where $\mathbf{A}_0$ represents the bulk-parameter supermatrix whose elements are

$$\mathbf{d}=\mathbf{f}_n/|v(\mathbf{k}_\parallel)| \text{ and } \tau=\sqrt{v(-\mathbf{k}_\parallel)/v(\mathbf{k}_\parallel)}\mathbf{I}_2, \tag{38}$$

where $\mathbf{f}_n$ is a 2×2 matrix defined as $\mathbf{f}_n=\Theta_n^{-1}\Lambda_n$ and $\mathbf{I}_2$ is the 2×2 unit matrix. The matrix $\mathbf{\Delta}$, which describes the effect due to the surface, is also a supermatrix whose elements are 2×2 matrices defined as

$$\Delta_{i,i}=(\mathbf{f}_i-\mathbf{f}_n)/|v(\mathbf{k}_\parallel)|, \quad i=1,2, \tag{39}$$

and $\mathbf{\Phi}_{n'}$ is a column vector whose nth element is a two-component vector defined as $\mathbf{\Phi}_{n,n'}$.

In the AFM phase we proceed by eliminating the equations associated with an odd layer index n. Since our analysis in the nonuniaxial case is limited to a semi-infinite metamagnet there is no need to treat cases with N odd or even differently. The resulting system of equations can be expressed in supermatrix form, where the elements of the supermatrix $\mathbf{A}_0$ are now defined as

$$\mathbf{d}=\mathbf{\Gamma}\mathbf{f}_{2\mu}-2\mathbf{I}_2 \quad \text{and} \quad \boldsymbol{\tau}=(v(-\mathbf{k}_\parallel)/v(\mathbf{k}_\parallel))\mathbf{I}_2, \tag{40}$$

where

$$\mathbf{\Gamma}=\mathbf{f}_{2\mu+1}/|v(\mathbf{k}_\parallel)|^2. \tag{41}$$

In the AFM phase the perturbation matrix $\mathbf{\Delta}$ has a single nonvanishing 2×2 element defined as

$$\Delta_{1,1}=\mathbf{\Gamma}(\mathbf{f}_2-\mathbf{f}_{2\mu})-\mathbf{f}_{2\mu+1}\mathbf{f}_1^{-1}+\mathbf{I}_2, \tag{42}$$

and the nth element of the column vector $\mathbf{\Phi}_{n'}$ is defined as $\mathbf{\Phi}_{2n,n'}$.

If we define $\mathbf{B}=\mathbf{A}_0^{-1}$, then the spin-wave modes can be determined in both phases from the determinantal condition as defined formally in Eq. (25). The construction of the elements of $\mathbf{B}$ and the condition for physically acceptable solutions of the surface-mode problem are discussed in detail in Ref. 10. Due to the algebraic complexity, we carry out the calculations numerically and obtain spin-wave dispersion relations for certain special cases that we illustrate in the following section.

V. APPLICATION TO $FeBr_2$ AND $FeCl_2$

We now apply the results of the previous sections to the $S=1$ metamagnets $FeBr_2$ and $FeCl_2$. These materials have different crystal structures that lead to important differences in their spin-wave properties. The positions of the Fe^{2+} ions in both materials are depicted in Fig. 1. Both materials have the same trigonal arrangement of the magnetic Fe^{2+} ions within any particular layer, but they differ from one another because they have different stacking arrangements of the layers. In $FeBr_2$, the Fe^{2+} ions are stacked vertically above and below those in adjacent layers, whereas in $FeCl_2$ the layers are staggered with respect to each other.

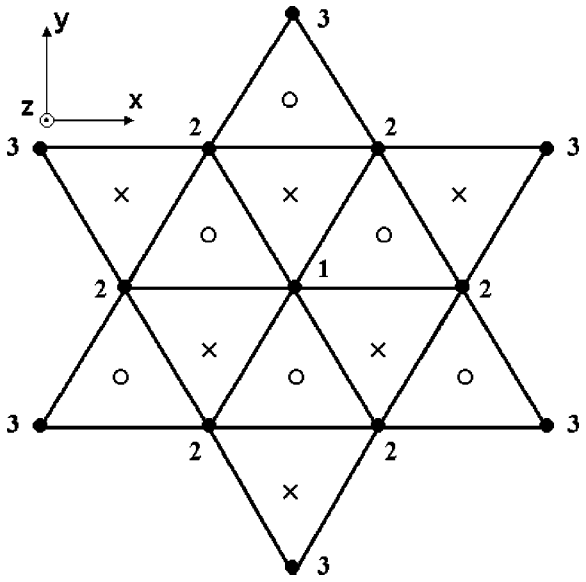

FIG. 1. Planar view of the Fe^{2+} ions (solid circles) in the ferromagnetically ordered layers for $FeBr_2$ and $FeCl_2$. The nearest and next-nearest neighbors to the ion labeled 1 are those labeled 2 and 3, respectively. The crosses and open circles represents the positions of the ions in the adjacent layers above and the below the planes for $FeCl_2$. For $FeBr_2$ the ions in adjacent layers are stacked vertically.

If we denote J_1 and J_2 as the nearest and next-nearest neighbor intralayer exchanges, respectively, the intralayer exchange sum defined in Eq. (8) is

$$u(\mathbf{k}_\parallel)=2J_1[\cos(k_xa)+2\cos(k_xa/2)\cos(k_ya\sqrt{3}/2)] + 2J_2[\cos(k_ya\sqrt{3})+2\cos(k_ya\sqrt{3}/2)\cos(k_xa3/2] \tag{43}$$

for both materials, where a is the nearest-neighbor distance in the layers. The interlayer exchange sum defined in Eq. (9) is simply $v(\mathbf{k}_\parallel)=J_3$ for $FeBr_2$, where J_3 denotes the interlayer nearest-neighbor exchange interaction. For $FeCl_2$ the interlayer exchange sum is

$$v(\mathbf{k}_\parallel)=J_3[\exp(ik_ya/\sqrt{3})+2\cos(k_xa/2)\exp(-ik_ya/2\sqrt{3})]. \tag{44}$$

The latter sum is more complicated because of the stacking arrangements of the layers in this case.

The approximate values for the exchange and anisotropy parameters for $FeBr_2$ and $FeCl_2$ have been determined using neutron-scattering and Raman-scattering experiments.[11–14] The values used in this work are listed in Table I. In the uniaxial case we set $F=0$.

Numerical calculations of the predicted spin-wave dispersion relations for $FeBr_2$ and $FeCl_2$ in the FM phase in the uniaxial approximation are shown in Figs. 2 and 3, respectively. We plot frequency versus in-plane wave vector k_xa (taking $k_y=0$) for an applied field corresponding to $h=4$ cm^{-1}, and evaluate thermal averages at $T/T_c=0.5$. In a semi-infinite system the bulk spin-waves appear as a band because of the range of values of the third wave vector component k_z. For a system with a finite number of layers N there

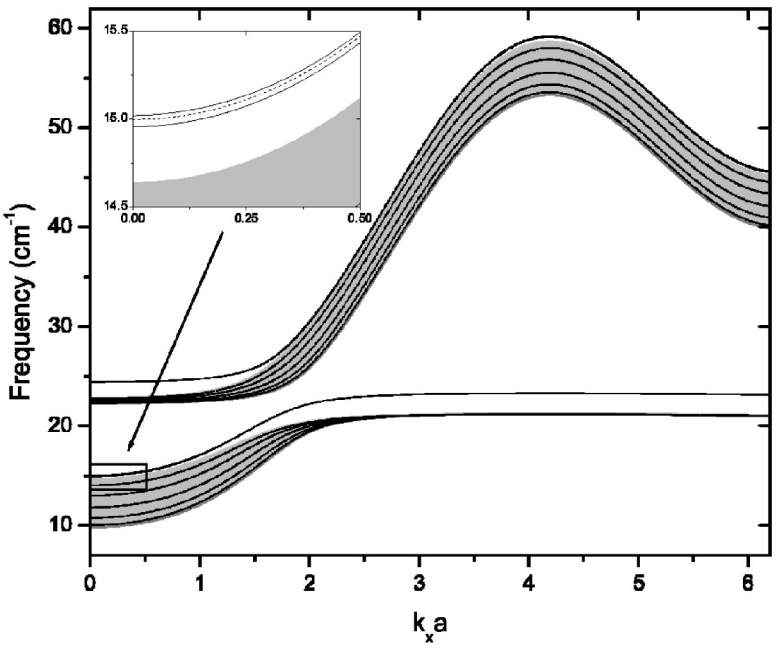

FIG. 2. The spin-wave frequencies (solid lines) plotted against in-plane wave vector $k_x a$ for a uniaxial ($F=0$) metamagnetic film of $FeBr_2$ in the FM phase. Here we have chosen $N=6$, $h=4$ cm^{-1}, and thermal averages at $T/T_c=0.5$. The shaded areas represent the bulk bands in the semi-infinite limit. The dotted line represents an acoustic surface spin-wave mode for a semi-infinite metamagnet.

is a restriction on the allowed values of k_z, which leads to discrete bulk spin-wave frequencies. The inclusion of thermal averages leads to a mode splitting effect between the acoustic and the additional optical spin-wave branches. The optical branches are absent in the low-temperature limit because there is no spectral weight associated with these modes. In the FM phase the acoustic and optical surface spin-wave branches are located above their respective bulk frequency bands. The inset in both figures focuses on the small wave vector region above the acoustic bulk band. Here the dotted line is the predicted surface mode in the semi-infinite limit, whereas the solid lines represent surface modes for the thin films. In both cases we predict an additional acoustic surface spin-wave branch when the number of layers N is finite. However, for $FeCl_2$ the splitting between one of the surface branches and the acoustic bulk region is extremely small.

In Figs. 4 and 5 we show the predicted bulk and surface dispersion relations for $FeBr_2$ in the AFM phase for the cases of the wave vector $\mathbf{k}_\parallel$ along the x and y directions, respectively. In both cases we take an applied field $h=0$, evaluate thermal averages at $T/T_c=0.5$, and consider results in the uniaxial limit ($F=0$). In the AFM phase the bulk regions are very narrow because the dependence on k_z is almost negligible. We only show results for a semi-infinite system because the splitting of the spin-wave modes in thin films is extremely small. Again, thermal effects produce a mode splitting between the acoustic and the optical spin-wave branches. In the AFM phase the acoustic and optical surface branches appear below their respective bulk bands by about 2 cm^{-1}. This splitting is sufficiently large to be observed using Raman scattering. Qualitatively similar results are obtained for $FeCl_2$. We only show the positive-frequency solutions, but there are some interesting effects on the spin-wave spectra as a result of the different symmetry properties of the metamagnetic films in the AFM phase. For a film with an odd number of layers N, the surfaces belong to the same sublattice and are equivalent. In the absence of an applied field (taking $h=0$), the spin-wave frequencies are nondegenerate and only positive-frequency surface modes are found. For $T>0$ we find one positive-frequency acoustic and optical surface mode. For a film with an even number of layers

TABLE I. Exchange and anisotrophy parameters used in calculations for $FeBr_2$ and $FeCl_2$.

	$FeBr_2$	$FeCl_2$
J_1 (cm^{-1})	5.07	5.5
J_2 (cm^{-1})	−1.2	−1.2
J_3 (cm^{-1})	1.45	0.28
D (cm^{-1})	7.34	9.4
F (cm^{-1})	2.0	2.0
$\sigma=\sigma'$	0.28	0.20

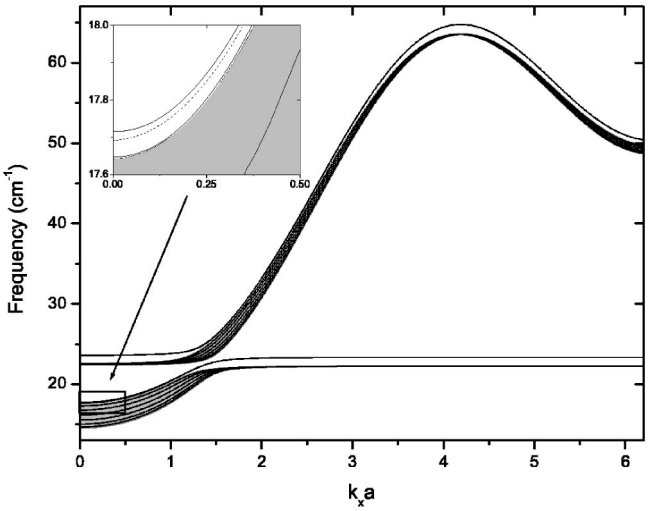

FIG. 3. The same as in Fig. 2, but for $FeCl_2$ and taking $N=8$.

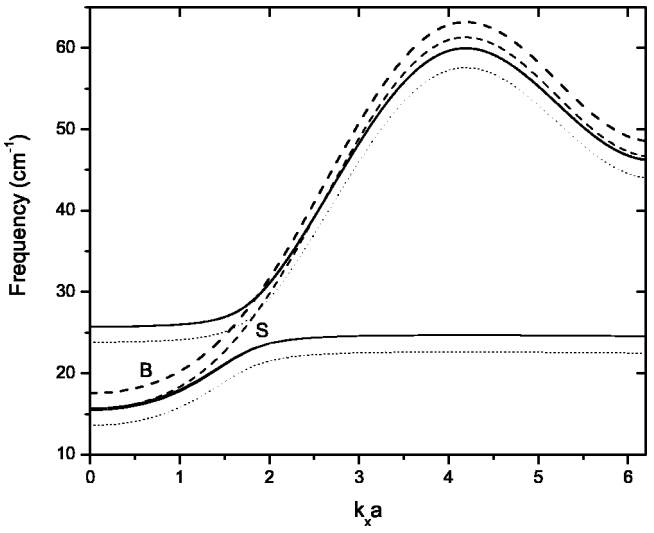

FIG. 4. The frequencies of bulk (shaded areas) and surface (dotted lines) spin waves for the semi-infinite uniaxial metamagnet $FeBr_2$ in the AFM phase plotted against in-plane wave vector $k_x a$ taking $h=0$ and thermal averages at $T/T_c=0.5$. The dashed lines labeled B and S represent, respectively, the bulk and surface spin-wave frequencies in the $T \ll T_c$ limit, where effects due to optical modes vanish.

N, the two sublattices are equivalent when $h=0$ and the spin-wave frequency spectrum is completely symmetric.

For comparison we also include in Figs. 4 and 5 the bulk (B) and surface (S) spin-wave frequencies as obtained in Ref. 5 for the $T \ll T_c$ limit. These results are obtained by representing the uniaxial anisotropy in terms of an effective anisotropy field. This approximation simplifies the spin dynamics by neglecting optical magnons and as a result there is no mode splitting observed. Identical results in the $T \ll T_c$ limit can be obtained using the commonly employed approach of transforming the spin operators to boson operators in a uniaxial approximation. Thermal effects are seen to produce

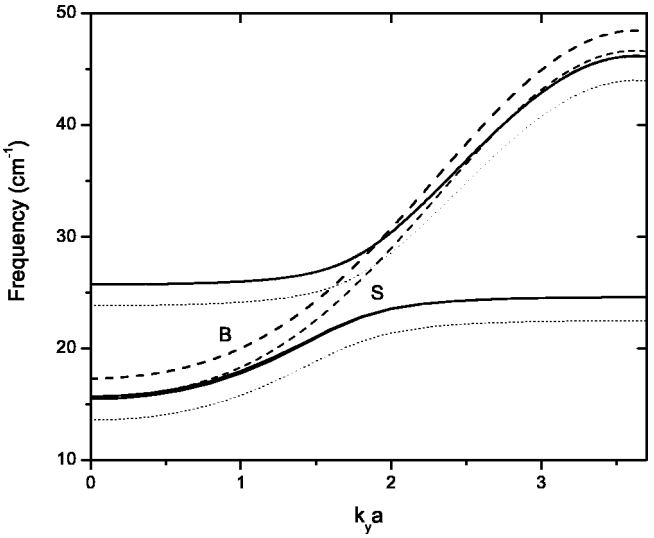

FIG. 5. The same as in Fig. 4, but with $\mathbf{k}_\parallel$ along the y direction.

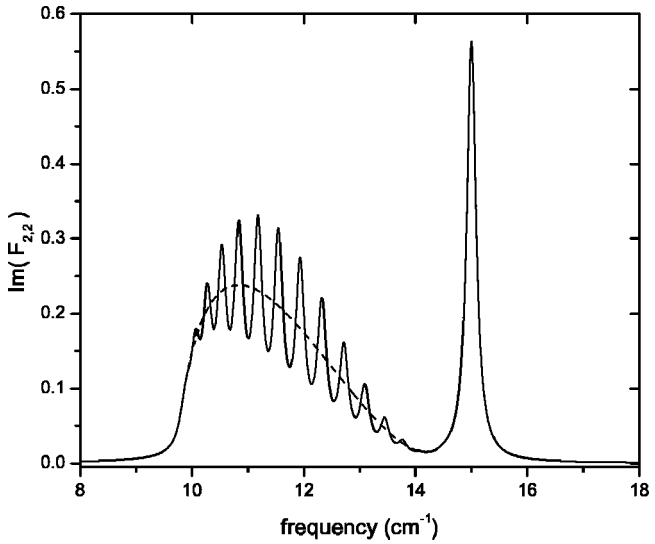

FIG. 6. Im($\mathbf{F}_{2,2}$) versus frequency for $FeBr_2$ in the FM phase. We compare the semi-infinite case (dashed line) to a film composed of 20 layers (solid line). We take $\mathbf{k} \approx 0$, $F=0$, $h=4.0$ cm^{-1}, $\eta=0.1$, and thermal averages at $T/T_c=0.5$. We show results for the lower (acoustic) frequency range.

a strong mixing between the acoustic and optical spin-wave branches and also lead to a renormalization of the spin-wave energies. Qualitatively similar results are obtained in the FM phase.

In Figs. 6 and 7 we show representative plots for $\mathrm{Im}[\mathbf{F}_{n,n}(\mathbf{k}_\parallel, \omega + i\eta)]$ versus frequency in the FM phase. Here we choose $n=2$, set $\mathbf{k}_\parallel \approx 0$ and $h=0$, take thermal averages at $T/T_c=0.5$, and compare results for the semi-infinite case to a film composed of 20 layers. In Fig. 6 we show results in the acoustic frequency range, whereas in Fig. 7 we show results in the optical frequency range. The peaks located at approximately 15 and 25 cm^{-1} are those associated with acoustic and optical surface modes, respectively. These attenuate rapidly with distance from the surfaces. As the temperature is increased the positions of the peaks renormalize to lower frequencies. The bulk acoustic and optical spin-wave frequency bands are broad because of the dependence of the third wavevector component k_z in the FM phase. In the AFM phase the acoustic and optical bulk regions are much narrowerbecause of a weak dependence on k_z. These effects are also seen in the dispersion relations.

In Table II we show numerical results for the layer-dependent mean-square amplitudes of spin waves in $FeBr_2$ in the AFM phase for different temperatures. The mean-square amplitudes associated with acoustic and optical surface modes in the surface layer $n=1$ are denoted by $Q_S^{ac}(1)$ and $Q_S^{op}(1)$, respectively. For acoustic and optical bulk spin-waves the mean-square amplitudes are denoted by $Q_B^{ac}(n)$ and $Q_B^{op}(n)$ and represent the contribution of all the modes within their respective bulk bands. The numerial results are obtained for a semi-infinite system in the small wave vector limit $\mathbf{k}_\parallel \approx 0$, taking $h=0$. We find that the mean-square amplitudes of the optical surface and bulk modes vanish in the low-temperature limit, as expected, but become important at elevated temperatures. In the AFM phase we also find that

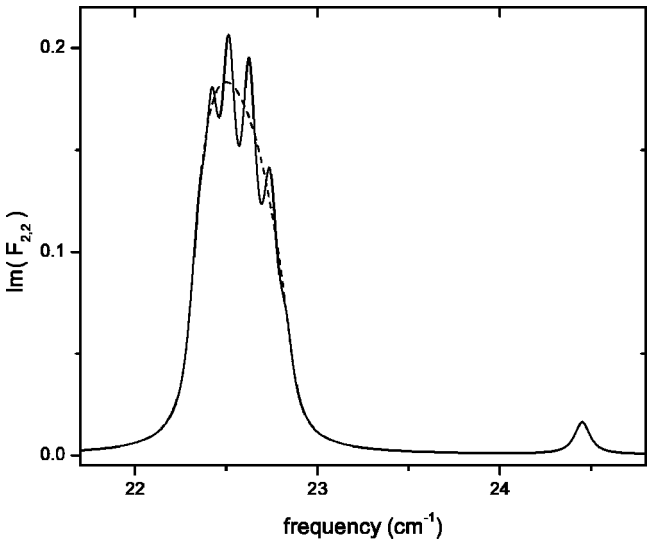

FIG. 7. The same as Fig. 6, except we take $\eta=0.05$ and show results for the higher (optical) frequency range.

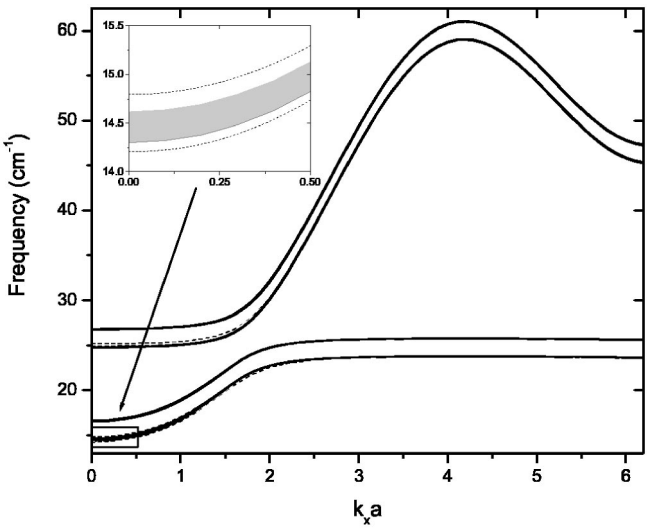

FIG. 8. The frequency of bulk (shaded areas) and surface (dashed lines) spin waves for the nonuniaxial metamagnet $FeBr_2$ in the AFM phase plotted against in-plane wave vector $k_x a$, taking $h=1.0$ cm^{-1} and evaluating thermal averages at $T/T_c=0.5$.

the positive-frequency modes have a greater precessional amplitude on the spin-up sublattice then on the spin-down sublattice. The converse is true for the negative-frequency (oppositely precessing) modes. In the FM phase the mean-square amplitudes associated with optical modes are significantly smaller then those for acoustic modes.

Figure 8 shows the dispersion relation of bulk and surface spin waves for the nonuniaxial metamagnet $FeBr_2$ in the AFM phase. Comparison of this spectrum with those for a uniaxial metamagnet shows that each bulk band is now split, giving rise to four separated bulk regions. In the absence of an applied field, this splitting is limited to the small wave vector region. The inclusion of the nonuniaxial anisotropy also leads to a splitting of the acoustic and optical surface modes. We find surface branches above and below the lowest frequency bulk band as well as two surface branches located between the higher energy bulk bands. In the nonuniaxial case the splitting between the surface branches and the bulk bands is small. In the FM phase the inclusion of the nonuniaxial anisotropy leads to modified spin-wave frequencies, but does not produce the additional splitting effects observed in the AFM phase.

VI. CONCLUSIONS

In this paper we have investigated thermal properties of surface and bulk spin waves in $S=1$ metamagnets. We have generalized previous results to higher temperatures by considering layer-dependent thermal averages for the spins and have considered spin waves in ultrathin films as well as in thicker films. We have considered the effects of uniaxial and nonuniaxial single-ion anisotropy and have examined spin-wave properties for metamagnets in both the AFM and FM phases. The method of calculation involved using a Green's function equation of motion formalism in which the anisotropy terms were treated exactly while the exchange-dependent terms were decoupled using RPA. We calculated the spin-wave dispersion relations and using appropriate correlation functions we evaluated the mean-square amplitude of spin precession.

TABLE II. Relative mean-square amplitudes of surface and bulk modes in the AFM phase for $FeBr_2$ for different temperatures (taking $\mathbf{k}_\parallel \approx 0$). Results are normalized to $Q_B^{ac}(10)$ at $T/T_c=0$.

T/T_c	0	0.3	0.5
$Q_S^{ac}(1)$	1.0	1.07	1.24
$Q_B^{ac}(10)$	1.0	1.06	1.19
$Q_S^{op}(1)$	0	0.03	0.15
$Q_B^{op}(10)$	0	0.03	0.14

Numerical results were obtained for the metamagnets $FeBr_2$ and $FeCl_2$, which have different crystal structures as well as different exchange and anisotropy parameters. At elevated temperatures, the use of modified thermal averages for the spins leads to additional optical magnetic excitations that correspond to transitions between the higher energy magnetic states and also produces a mode splitting effect between the acoustic and the additional optical spin-wave branches. This splitting vanishes in the low-temperature limit because there is no statistical weight associated with the optical spin waves. The layer-dependent mean-square amplitudes of the spin precession for optical surface and bulk modes are negligible in the low-temperature limit but become important at elevated temperatures. The nonuniaxial anisotropy leads to additional splitting of the surface and bulk spin-wave branches.

These predicted features could be investigated experimentally using inelastic light scattering techniques such as Raman and Brillouin scattering and magnetic resonance. For the study of surface excitations using light scattering it would be appropriate to use an excitation wavelength for which the metamagnets are optically opaque and use a scattering geometry that enhances surface effects. Metamagnetic materials in the AFM phase would be the best candidates for experimental studies because our theoretical predictions in-

dicate that there is a sufficiently large spacing between surface and bulk spin-wave modes and the mean square amplitudes of spin precession (which we use as measure of intensity) are the largest in this phase.

ACKNOWLEDGMENT

The authors are grateful to NSERC (of Canada) for support of this project.

APPENDIX A: THERMAL AVERAGES

We now briefly discuss the approximate evaluation of the static thermal averages using a modified mean-field theory. Although the thermal averages can, in principle, be calculated self-consistently using the Green's functions, and their correlation functions, this becomes rather complicated for the general nonuniaxial case $F \neq 0$. Instead, we employ a modified mean-field approximation to simplify the exchange terms in the Hamiltonian (see Ref. 16), but we treat the anisotropy terms exactly.

The thermal average $\langle X \rangle$ of an operator X in any representation can be written as

$$\langle X \rangle = \mathrm{Tr}[X \exp(-\beta H)]/\mathrm{Tr}[\exp(-\beta H)]. \tag{A1}$$

We evaluate the various thermal averages using the following mean-field Hamiltonian

$$H_{MF} = -\sum_i B_e(i) S_i^z - D[\sum_i (S_i^z)^2 + \sum_j (S_j^z)^2] - F[\sum_i (S_i^x)^2 - (S_i^y)^2], \tag{A2}$$

where $B_e(i) = h - h_e(i) + h_e'(i)$ and the effective interlayer and intralayer exchange fields are, respectively,

$$h_e(i) = (1+\sigma)\sum_j \langle S_j^z \rangle J_{i,j}, \tag{A3}$$

$$h_e'(i) = (1+\sigma')\sum_{i'} \langle S_{i'}^z \rangle J_{i,i'}'. \tag{A4}$$

The applied field h is assumed to be in the z-direction.

It is clear from symmetry considerations that the effective exchange fields along with the thermal averages depend on position only through the layer index n. The effective intralayer exchange field is the same for both $FeBr_2$ and $FeCl_2$ because they have identical structures within any particular layer, and is written as $h_e'(n) = 6(J_1 + J_2)\langle S^z \rangle_n (1+\sigma')$.

Spins in surface layers $n=1$ and $n=N$ have p ($p=1$ for $FeBr_2$, $p=3$ for $FeCl_2$) interlayer nearest neighbor, and the effective interlayer fields for the surface layers are

$$h_e(1) = pJ_3 \langle S^z \rangle_2 (1+\sigma), \quad n=1, \tag{A5}$$

$$h_e(N) = pJ_3 \langle S^z \rangle_{N-1} (1+\sigma), \quad n=N. \tag{A6}$$

For interior layers ($1 < n < N$), we have

$$h_e(n) = pJ_3 (\langle S^z \rangle_{n-1} + \langle S^z \rangle_{n+1})(1+\sigma). \tag{A7}$$

For a spin $S=1$ system, we employ the 3×3 irreducible representation for the spin operators and write down the 3×3 matrix for the effective Hamiltonian H_{MF}. In the uniaxial case ($F=0$), the Hamiltonian is diagonal and the calculation of the thermal averages is straightforward. In the nonuniaxial case ($F \neq 0$), H_{MF} is nondiagonal, but may be diagonalized by the transformation

$$\tilde{H}_{MF} = \mathbf{U}^{-1} H_{MF} \mathbf{U}, \tag{A8}$$

where the columns of the matrix $\mathbf{U}$ are the normalized eigenvectors of H_{MF}. The thermal averages are evaluated using

$$\langle X \rangle_n = \mathrm{Tr}[\tilde{X}_i \exp(-\beta \tilde{H}_{MF})]/\mathrm{Tr}[\exp(-\beta \tilde{H}_{MF})], \tag{A9}$$

with $\tilde{X}_i = \mathbf{U}^{-1} X_i \mathbf{U}$. Replacing the operator X_i with S_i^z, $(S_i^z)^2$ and $(S_i^+)^2$, we obtain a set of recurrence relationships satisfied by the various thermal averages for $n = 1, \ldots, N$. Finally, the layer-dependent thermal averages are

$$\langle S^z \rangle_n = \frac{B_e(n)[\exp(Z\beta) - \exp(-Z\beta)]}{Z[\exp(Z\beta) - \exp(-Z\beta) + \exp(-D\beta)]},$$

$$\langle (S^z)^2 \rangle_n = \frac{[\exp(Z\beta) - \exp(-Z\beta)]}{[\exp(Z\beta) - \exp(-Z\beta) + \exp(-D\beta)]}, \tag{A10}$$

$$\langle (S^+)^2 \rangle_n = \frac{F \langle S^z \rangle_n}{B_e(n)},$$

where $Z = \sqrt{B_e(n)^2 + F^2}$. Note that in the uniaxial case ($F=0$) the thermal average $\langle (S^+)^2 \rangle_n$ is zero.

*Electronic address: cottam@uwo.ca

[1] J. A. C. Bland and B. Heinrich, *Ultrathin Magnetic Structures I* (Springer Verlag, Berlin, 1994).

[2] *Linear and Nonlinear Spin Waves in Magnetic Films and Superlattices*, edited by M. G. Cottam (World Scientific, Singapore, 1994).

[3] P. Grünberg, in *Light Scattering in Solids V*, edited by M. Cardona and G. Güntherodt (Springer, Heidelberg, 1989), p. 303.

[4] M. G. Cottam and D. J. Lockwood, *Light Scattering in Magnetic Solids* (Wiley, New York, 1986) pp. 118–127.

[5] J. H. Baskey and M. G. Cottam, Phys. Rev. B **42**, 4304 (1990).

[6] D. H. A. L. Anselmo, E. L. Albuquerque, and M. G. Cottam, J. Appl. Phys. **83**, 6955 (1998).

[7] E. Meloche and M. G. Cottam, Phys. Status Solidi A **196**, 165 (2003).

[8] N. Zubarev, Sov. Phys. Usp. **3**, 320 (1960).

[9] J. M. Pereira and M. G. Cottam, Phys. Rev. B **63**, 174431 (2001).

[10] T. Wolfram and R. E. De Wames, Phys. Rev. **185**, 762 (1969).

[11] W. B. Yelon and C. Vettier, J. Phys. C **8**, 2760 (1975).
[12] D. J. Lockwood, G. Mischler, A. Zwick, I. W. Johnstone, G. C. Psaltakis, M. G. Cottam, S. Legrand, and J. Leotin, J. Phys. C **15**, 2793 (1982).
[13] M. G. Pini, E. Rastelli, A. Tassi, and V. Tognetti, J. Phys. C **14**, 3041 (1981).
[14] G. C. Psaltakis and M. G. Cottam, J. Phys. C **15**, 4847 (1982).
[15] M. G. Cottam and D. Kontos, J. Phys. C **13**, 2945 (1980).
[16] M. G. Cottam and D. R. Tilley, *Introduction to Surface and Superlattice Excitations* (Cambridge University Press, Cambridge, 1989), pp. 91–92.